Heme Complexes

DOI: 10.1002/anie.201108691

Guanidine-Ferroheme Coordination in the Mutant Protein Nitrophorin 4(L130R)**

Chunmao He, Martin R. Fuchs, Hideaki Ogata, and Markus Knipp**

The Arg130:N^{ω} atom coordinates the heme iron atom in the novel L130R mutant of the heme protein nitrophorin 4 (NP4) at low temperature. NP4 is a ferriheme protein that is found in the saliva of the blood-sucking insect *Rhodnius prolixus*. X-ray structures reveal that its architecture resembles the antiparallel 8-stranded β-barrel body structure of the lipocalins.[1] The heme *b* cofactor, which is typically in the ferriheme state, is embedded in the barrel and concomitantly coordinated by His59:N^{τ}. The distal iron coordination site is not occupied by an amino acid. Instead, it is ready to bind a number of low-molecular weight ligands, including water, NO, NO_2^-, CN^-, and imidazole (ImH).[2] While studying the mechanism of the reaction of NP4 with NO_2^-,[3] we generated a mutant protein NP4(L130R) with surprising characteristics that we present herein.

The choice for the mutation of the distal pocket Leu130 residue was made upon careful inspection of the X-ray structures. It was noticed that this side-chain, which is part of the flexible G-H loop, should have ample space to not disturbing the fold upon mutation.[4,5] The expression and purification of NP4(L130R) yields quantities of protein comparable to that of wild type (wt) protein. The absorbance spectra (Figure S1, Supporting Information) and resonance Raman (RR) spectra (Figure S2, Supporting Information) are very similar to those of the wt protein indicating a 6-coordinate (6c) high-spin (HS) Fe^{III} complex ($S = {}^5/_2$), that is, with a distal water ligand. This situation is in good agreement with the obtained axial cw-EPR spectrum shown in Figure 1, which is typical for HS ferriheme proteins with a weak distal ligand, such as wt NP4[3b] (Figure 1). However,

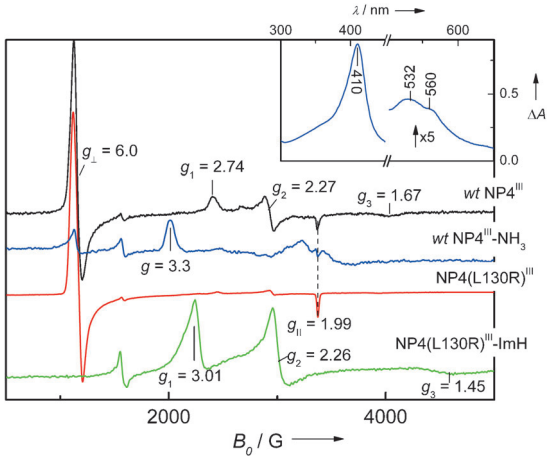

Figure 1. X-band EPR spectra of NP4 (black), NP4[NH_3] (blue), NP4-(L130R) (red), and NP4(L130R)[ImH] (green). Spectra were recorded at 10 K. All samples were in 100 mM HEPES/NaOH, 25% glycerol (pH 7.2) except for NP4[NH_3], which was in 2 M NH_4OAc, 100 mM MOPS/NaOH (pH 7.5). Inset: Absorbance spectrum of NP4[NH_3] in 2 M NH_4OAc, 100 mM MOPS/NaOH (pH 7.5) at ambient temperature. HEPES = 2-[4-(2-hydroxyethyl)-1-piperazinyl]ethanesulfonic acid, MOPS = 3-(4-morpholinyl)-1-propanesulfonic acid.

in the case of wt NP4 a significant contribution from a low-spin (LS) species is found, which is attributed to the OH^- complex as a consequence of partial deprotonation of the water ligand,[6] this deprotonation is virtually absent in case of NP4(L130R).

The large distal pocket of NPs allows the binding of rather bulky ligands, for example, ImH or histamine. Complexes with ImH are among the best characterized LS species ($S = {}^1/_2$) of NPs. Furthermore, the bulkiness of ImH in combination with the sensitivity of the *g* tensor to the rotational orientation relative to the heme $N_{pyrrole}$–Fe–$N_{pyrrole}$ axis[7] makes ImH a good probe with which to study the influence of the mutation by EPR spectroscopy. The cw-EPR spectrum of NP4(L130R)[ImH] is displayed in Figure 1. The principal *g* values are comparable to those reported for other NP[ImH] complexes as can be seen from Table 1. The slightly larger *g* strain of the mutant reflects some inhomogeneity with respect to the orientation of ImH on the heme plane.[7] Overall, NP4(L130R)[ImH] resembles the coordination geometry found for the wt structure.

Crystals of NP4(L130R) appear after around 2 weeks using 3.2 M ammonium phosphate (pH 7.4) as a precipitant, which is similar to the conditions reported for wt NP4.[1,4,8] Crystals of NP4(L130R)[ImH] were prepared by soaking NP4(L130R) crystals in mother liquor containing 10 mM of ImH prior to freezing. Diffraction datasets were taken at

[*] C. He, Dr. H. Ogata, Dr. M. Knipp
Max-Planck-Institut für Bioanorganische Chemie
Stiftstrasse 34–36, 45470 Mülheim an der Ruhr (Germany)
E-mail: ogata@mpi-muelheim.mpg.de
mknipp@mpi-muelheim.mpg.de
Dr. M. R. Fuchs
Swiss Light Source, Paul-Scherrer-Institut
5232 Villigen (Switzerland)

[**] The technical assistance of Yvonne Brandenburger, Jan Hanis, Robyn L. Kosinsky, Koji Nishikawa, Alina Steinbach, Johanna J. Taing, and the staff of beamline BL14.2 at BESSYII (Helmholtz-Zentrum Berlin (Germany)) as well as Florian Dworkowski and Guillaume Pompidor of the Spectrolab facility at beamline X10SA of the Swiss Light Source is acknowledged. Further, we thank F. Ann Walker (University of Arizona, Tucson, AZ) for the NP4 expression plasmid. This work was financially supported by the Max Planck Society (MPG) and by the Deutsche Forschungsgemeinschaft (DFG), Grant KN 951-1/1 and KN 951-1/2 (to M.K.).

Supporting information for this article is available on the WWW under http://dx.doi.org/10.1002/anie.201108691.

Table 1: The principal *g* values of the ImH complex of NP4(L130R) and of wt NP4, -2, and -7.

Species	g_1	g_2	g_3	Reference
NP4(L130R)	3.01	2.26	1.45	This work
wt NP4	3.02	2.25	1.46	[9]
wt NP2	3.02	2.26	1.37	[10]
wt NP7	3.07	2.19	1.36	[11]

100 K and the crystal structures of NP4(L130R) and NP4-(L130R)[ImH] were solved by molecular replacement at a resolution of 1.3 and 1.4 Å, respectively. The crystallographic refinement parameters are summarized in Table S1 in the Supporting information and a comparison of the overall structures of NP4(L130R) and NP4(L130R)[ImH] with those of the respective wt protein structures is presented in Figure S3 and S4 of the Supporting Information. Overall, the influence of the mutation on the total structure is negligible as is indicated by the high degree of structural similarity between NP4 and NP4(L130R) (root-mean squared deviation (RMSD) = 0.49 Å) and between NP4[ImH] and NP4(L130R)[ImH] (RMSD = 0.69 Å).

A detailed representation of the heme pockets of NP4-(L130R)[ImH] and NP4(L130R) is shown in Figure 2. In case of NP4(L130R)[ImH] a single crystal form was obtained with very similar structural features to wt NP4[ImH].[12] Similar to Leu130 in the wt, the Arg130 side-chain is folded towards the front of the distal heme pocket and does not interfere with the ImH ligand. The similarity between the heme pockets is also reflected by the comparable degree of distortion of the heme planarity (Supporting Information, Figure S5).

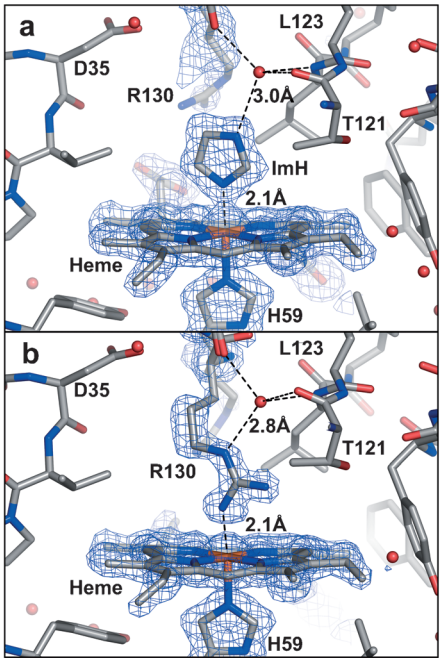

Figure 2. The $2F_o-F_c$ electron density map (contour level: 1σ) of the heme pocket of NP4, a) NP4(L130R)[ImH] (PDB code: 3TGB) and b) NP4(L130R) (PDB code: 3TGA). The electron density map covers the heme and the residues His59 and Arg130.

In the heme pocket of NP4(L130R), Arg130 adopts two conformations (Supporting Information, Figure S3). Surprisingly, in the form with the higher occupancy (ca. 60%), the iron is axially coordinated by Arg130:N^{ω} with an interatomic distance of 2.1 Å (Figure 2B). To our knowledge, this is the first example of an Arg-coordinated metalloporphyrin. The crystallographic results are surprising because the spectroscopic data do not give evidence for a strong interaction of Arg130:N^{ω} with the iron center, whereas the bond length suggests a strong interaction.

Examples of coordination complexes with guanidine ligands are scarce, and in biomolecules nearly unknown.[13] A big challenge for their formation is the high pK_a value of guanidines (for example, arginine ca. 12.5), so that in aqueous media their deprotonation is hardly achieved.[13c] Metal complexes of guanidines have been reported for Cr^{II}, Mn^{II}, Fe^{II}, Co^{II}, Ni^{II}, $Cu^{I/II}$, Zn^{II}, Pd^{II}, Pt^{II}, and Au^{I} and in all cases the coordination is through the imine nitrogen atom.[13,14] By analogy, the C=N^{ω}(H)–Fe coordination should occur through the N^{ω} lone pair. The C–N^{ω}H(Fe) distance (1.32 Å) is indeed slightly smaller than the C–$N^{\omega}H_2$ distance (1.33 Å), although this is at the edge of the resolution. However, of the approximately 150 guanidine-metal interactions deposited in the Cambridge Structural Database (CSD) most are diguanidines and only four examples of individual guanidine–metal interactions are reported.[13d] The few examples of protein structures containing Arg:N^{ω}–metal bonds are the arginase of *Bacillus caldovelox* (Mn)[15] and a human carbonic anhydrase variant (Zn).[16] Most interesting in this context is the Arg coordination of one of the iron atoms in the [2Fe-2S] cluster of biotin synthase BioB,[13e,17] not least because very few iron–guanidine complexes are known at all.[13b,14a,e,f] However, the rather poor resolution of this structure (3.4 Å, protein data bank (PDB) code: 1R30) does not provide reliable bond parameters. Recent QM/MM calculations on four models of this site support the C=N^{ω}(H)–Fe arrangement.[13e] Overall, the N^{ω}–Fe distance is slightly longer than the mean $N_{guanidine}$–M^{n+} distance of 1.91 ± 0.06 Å found in the synthetic guanidine complexes[13d] but is very similar to the N^{ω}–Fe distance in the complex $[Fe(TMG_3tren)NCCH_3]^{2+}$ (2.07–2.25 Å; TMG_3tren = tris(tetramethylguanidino)tren; with tren = tris(2-aminoethyl))[13b] and distances calculated for the BioB [2Fe-2S] cluster models (2.05–2.18 Å).[13e] The angle ∡(C=N^{ω}–Fe) of 141° is wider than the mean ∡(C=N–M^{n+}) angle of 129 ± 2°, which is probably a consequence of the constraints of the protein structure. The dihedral angle ∡(N^{δ}–C=N^{ω}–Fe) of 0° is close to the mean angle in guanidine–metal compounds of ∡(RNH–C=N–M^{n+}) = −1 ± 9°.[13d]

Another aspect of the weakness of the bonding in guanidine–metal ion complexes is the negligible Lewis basicity.[13c] Of the few metal complexes reported, there is one complex of Fe^{II}, but not of Fe^{III}.[13b] Therefore, to determine whether Fe^{II} might be the coordinating entity in the NP4(L130R) crystals, X-ray irradiation of NP4(L130R) crystals was performed in conjunction with UV/Vis absorption using a microspectrophotometer attached to the beam line.[18] The initial absorbance spectrum of the crystal is depicted in Figure 3. It should be noted that in NP crystals grown in ammonium phosphate, NH_3 is available as a distal

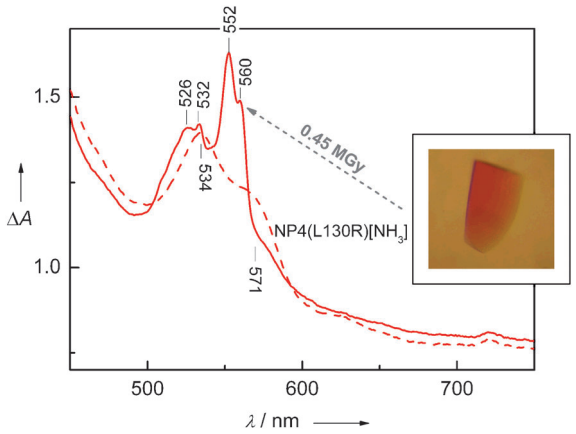

Figure 3. Absorbance spectrum of a crystal of NP4(L130R) grown in 3.2 M ammonium phosphate (pH 7.4) before (dashed line) and after (continuous line) X-ray irradiation. Inset: Single crystal of NP4(L130R).

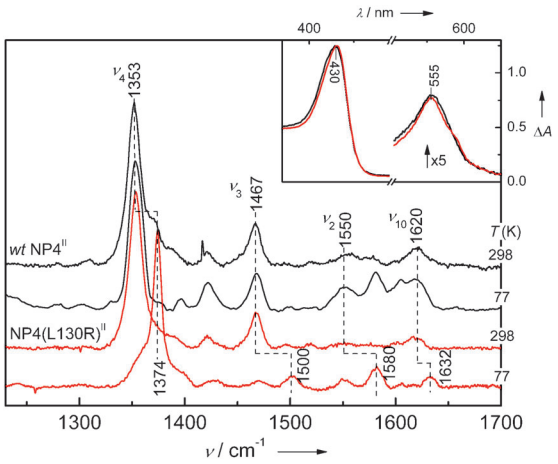

Figure 4. RR spectra of NP4 (black) and NP4(L130R) (red) in 100 mM HEPES/NaOH (pH 7.2) at ambient temperature and at 77 K (λ_{ex} = 413.1 nm). Inset: absorbance spectra of NP4[Fe^{II}] and NP4-(L130R)[Fe^{II}] at ambient temperature.

iron ligand. Although this has been proposed,[1,4,8,19] it was never demonstrated experimentally. Herein we show that the absorbance spectrum of the crystal resembles that of a LS complex, which is indicated by the two intense Q-bands. For comparison, an absorbance spectrum of NP4[NH_3] was recorded (Figure 1, top right). Also, the cw-EPR spectrum of this sample reveals a LS species as indicated by a highly anisotropic low-spin (HALS) signal with $g_{max} = 3.3$ (Figure 1).

The crystals were then irradiated by a low intensity X-ray beam (12.4 keV, 3.5×10^{10} photons s^{-1}) and spectra were sampled continuously over 5 min to a total dose of 0.45 MGy (Supporting Information, Figure S6 A). The kinetic trace in Figure S6 B shows that the photo reduction of the crystal is accomplished to 50 % within the first 0.2 MGy and a novel LS species is formed, as indicated by the two sharp Q-bands in Figure 3. The splitting in the absorbance bands reflects the concomitant presence of NP4(L130R)[Fe^{II}–N^{ω}_{R130}] (526, 552 nm) and NP4(L130R)[Fe^{II}–NH_3] (532, 560 nm), which is assigned by comparison with the spectra of NP4(L130R)[$Fe^{II/III}$–NH_3] in solution (Supporting Information, Figure S7). For comparison, the total dose applied during the collection of the dataset used for the solution of the structure of NP4(L130R) (Figure 2) was approximately 15-fold higher than the total dose for the spectral kinetic measurements. Therefore, the structure is of the ferroheme state NP4(L130R)[Fe^{II}–N^{ω}_{R130}].

However, at room temperature, the absorbance spectrum of ferroheme NP4(L130R) generated by careful chemical reduction with $Na_2S_2O_4$ (Figure 4, top right), is not different from that of NP4[Fe^{II}].[1,20] The high-frequency region (1200–1700 cm^{-1}) of the Soret band excited RR spectrum has a high diagnostic potential with regard to the coordination and spin-state of heme proteins.[21] The RR spectrum of NP4(L130R)-[Fe^{II}] at room temperature is identical to that of NP4[Fe^{II}] (Figure 4). Thus, the so-called oxidation-state marker band ν_4 is well in the range of ferrohemes (1350–1375 cm^{-1}).[21,22] The so-called coordination-state marker band ν_3 is sensitive to the heme core size, which changes with the spin state of the iron in a particular oxidation state, that is, 1460–1470 cm^{-1} for a 5cHS Fe^{II} and 1490–1510 cm^{-1} for a 5cLS or 6cLS Fe^{II} center.[22a,b,23] Consequently, NP4[Fe^{II}], like NP4(L130R)-[Fe^{II}], can be assigned as the expected 5cHS complex. In contrast, recording the RR spectra at 77 K reveals a significant change of ν_4 and ν_3 toward values indicative of LS for NP4(L130R)[Fe^{II}], in agreement with the absorbance spectrum of the frozen crystal (Figure 4). As a control, after these measurements samples were thawed and subjected to absorbance spectroscopy at room temperature, which revealed the HS species again. Thus, the temperature dependent HS⇄LS conversion in NP4(L130R)[Fe^{II}] is fully reversible. As expected, the coordination and spin-state of NP4[Fe^{II}] do not depend on temperature (Figure 4).

Scheme 1 summarizes the findings reported herein. The coordination of Arg130:N^{ω} to the heme iron center is highly dependent on the iron oxidation state (Fe^{II}) and on the temperature. An Fe^{II} center is a softer Lewis acid than Fe^{III}

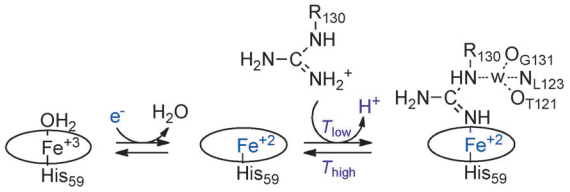

Scheme 1. Reaction scheme for the binding of the internal Arg130 guanidine to Fe^{II} in NP4(L130R). (w = water oxygen atom)

and is, therefore, expected to better coordinate the imine nitrogen atom. However, the reason for the temperature dependence is less obvious. The concomitant appearance of Arg130:N^{ω} coordination in the crystal state and in frozen solution rules out a crystallographic artifact from structural deformation during crystal growth. Another possibility may be the change in the pK_a value of Arg130 and/or the change of the pH value of the solution, both of which are temperature-dependent parameters, although, in principle, the pH value is not defined in a frozen solution. On the other hand, the

influence of temperature on coordination and spin state is sometimes observed. For example, in case of NP1[{FeNO}^{7}] ($S = {}^1/_2$) a mixture of 5c and 6c is detected by EPR spectroscopy at 4.2 K but not at room temperature in absorbance spectroscopy.[24] Furthermore, RR spectroscopy of NP1[Fe^{III}] at 298 K suggests 6cHS, that is, a bound water ligand is present, where at 77 K 6cLS is dominant.[25]

A number of heme proteins contain an Arg residue in the distal heme pocket site. A selection of those for which an X-ray structure is available and that have a meaningful Arg:N–Fe distance is presented in Table S2 of the Supporting Information. However, NP4(L130R) remains the only case in which an Arg:N$^{\omega}$–Fe bond occurs. Figure 2b shows that a water molecule is hydrogen bonded to Arg130:N$^{\delta}$(H) and three other backbone atoms. As can be seen from Figure 2a, this water is also present in NP4(L130R)[ImH], coordinated to the N^1(H) of ImH. It is also found in the structures of NP4[ImH] (PDB code: 1IKJ) and of NP4[histamine] (PDB code: 1IKE).[12] The orientation of the guanidine plane toward the heme $N_{pyrrole}$–Fe–$N_{pyrrole}$ axis is very similar to the orientation of ImH and histamine in the NP4 structures and the bond lengths and angles are comparable (see Table S3, Supporting Information). These data further support the imine N$^{\omega}$ coordination mode of Arg130 as does the similarity to the imine N^3 coordination of the imidazoles.

In conclusion, this study of the non-native protein variant NP4(L130R) shows that an iron guanidine bond in an iron porphyrin is in principle possible. It is remarkable that this was first achieved in a protein. The advantage of the protein matrix is undoubtedly that the overall structure ties the ligands together gaining binding energy from the chelate effect. Furthermore, guanidine deprotonation has to be accomplished, which is difficult in water but is assisted by the environment created by the heme pocket. The weak coordination is additionally stabilized through a water molecule. Moreover, stabilization was also achieved through low temperature and through reduction of the iron.

Received: December 9, 2011
Published online: February 14, 2012

Keywords: guanidine · heme complexes · nitrophorin · photoreduction · proteins

[1] E. M. Maes, S. A. Roberts, A. Weichsel, W. R. Montfort, *Biochemistry* **2005**, *44*, 12690 – 12699.
[2] a) F. A. Walker, *J. Inorg. Biochem.* **2005**, *99*, 216 – 236; b) M. Knipp, C. He, *IUBMB Life* **2011**, *63*, 304 – 312.
[3] a) C. He, M. Knipp, *J. Am. Chem. Soc.* **2009**, *131*, 12042 – 12043; b) C. He, H. Ogata, M. Knipp, *Biochemistry* **2010**, *49*, 5841 – 5851.
[4] E. M. Maes, A. Weichsel, J. F. Andersen, D. Shepley, W. R. Montfort, *Biochemistry* **2004**, *43*, 6679 – 6690.
[5] Two other distal pocket Leu residues, Leu123 and Leu133, have a major impact on the heme distortion and, thus, reduction potential. T. K. Shokhireva, R. E. Berry, E. Uno, C. A. Balfour, H. Zhang, F. A. Walker, *Proc. Natl. Acad. Sci. USA* **2003**, *100*, 3778 – 3783.
[6] This was determined by pH titration (unpublished results C.H. and M.K.). It was already shown for NP2 and NP3 that the pK_a values of the ligand water is relatively low, ca. 10.1 and 9.2, respectively. T. K. Shokhireva, R. E. Berry, H. Zhang, N. V. Shokhirev, F. A. Walker, *Inorg. Chim. Acta* **2008**, *361*, 925 – 940.
[7] a) F. A. Walker, *Chem. Rev.* **2004**, *104*, 589 – 615; b) F. A. Walker, *Coord. Chem. Rev.* **1999**, *185 – 186*, 471 – 534.
[8] M. Schmidt, K. Achterhold, V. Prusakov, F. G. Parak, *Eur. Biophys. J.* **2009**, *38*, 687 – 700.
[9] R. E. Berry, X. D. Ding, T. K. Shokhireva, A. Weichsel, W. R. Montfort, F. A. Walker, *J. Biol. Inorg. Chem.* **2004**, *9*, 135 – 144.
[10] T. K. Shokhireva, N. V. Shokhirev, F. A. Walker, *Biochemistry* **2003**, *42*, 679 – 693.
[11] M. Knipp, F. Yang, R. E. Berry, H. Zhang, M. N. Shokhirev, F. A. Walker, *Biochemistry* **2007**, *46*, 13254 – 13268.
[12] S. A. Roberts, A. Weichsel, Y. Qiu, J. A. Shelnutt, F. A. Walker, W. R. Montfort, *Biochemistry* **2001**, *40*, 11327 – 11337.
[13] a) E. M. A. Ratilla, N. M. Kostić, *J. Am. Chem. Soc.* **1988**, *110*, 4427 – 4428; b) H. Wittmann, V. Raab, A. Schorm, J. Planckmeyer, J. Sundermeyer, *Eur. J. Inorg. Chem.* **2001**, 1937 – 1948; c) P. J. Bailey, S. Pace, *Coord. Chem. Rev.* **2001**, *214*, 91 – 141; d) L. Di Costanzo, L. V. Flores, Jr., D. W. Christianson, *Proteins Struct. Funct. Genet.* **2006**, *65*, 637 – 642; e) M. G. G. Fuchs, F. Meyer, U. Ryde, *J. Biol. Inorg. Chem.* **2010**, *15*, 203 – 212.
[14] a) S. Pohl, M. Harmjanz, J. Schneider, W. Saak, G. Henkel, *J. Chem. Soc. Dalton Trans.* **2000**, 3473 – 3479; b) A. Neuba, S. Herres-Pawlis, U. Flörke, G. Henkel, *Z. Anorg. Allg. Chem.* **2008**, *634*, 771 – 777; c) S. Herres-Pawlis, U. Flörke, G. Henkel, *Eur. J. Inorg. Chem.* **2005**, 3815 – 3824; d) A. Neuba, R. Haase, M. Bernard, U. Flörke, S. Herres-Pawlis, *Z. Anorg. Allg. Chem.* **2008**, *634*, 2511 – 2517; e) F. A. Cotton, C. A. Murillo, D. J. Timmons, *Polyhedron* **1999**, *18*, 423 – 428; f) S. H. Oakley, D. B. Soria, M. P. Coles, P. B. Hitchcock, *Polyhedron* **2006**, *25*, 1247 – 1255; g) M. P. Coles, *Dalton Trans.* **2006**, 985 – 1001.
[15] M. C. Bewley, P. D. Jaffrey, M. L. Patchett, Z. F. Kanyo, E. N. Baker, *Structure* **1999**, *7*, 435 – 448.
[16] M. Ferraroni, S. Tilli, F. Briganti, W. R. Chegwidden, C. T. Supuran, K. E. Wiebauer, R. E. Tashian, A. Scozzafava, *Biochemistry* **2002**, *41*, 6237 – 6244.
[17] a) R. B. Broach, J. T. Jarrett, *Biochemistry* **2006**, *45*, 14166 – 14174; b) F. Berkovitch, Y. Nicolet, J. T. Wan, J. T. Jarrett, C. L. Drennan, *Science* **2004**, *303*, 76 – 79.
[18] R. L. Owen, A. R. Pearson, A. Meents, P. Boehler, V. Thominet, C. Schulze-Briese, *J. Synchrotron Radiat.* **2009**, *16*, 173 – 182.
[19] D. A. Kondrashov, S. A. Roberts, A. Weichsel, W. R. Montfort, *Biochemistry* **2004**, *43*, 13637 – 13647.
[20] a) M. Knipp, J. J. Taing, C. He, *J. Inorg. Biochem.* **2011**, *105*, 1405 – 1412; b) C. He, S. Neya, M. Knipp, *Biochemistry* **2011**, *50*, 8559 – 8575.
[21] a) J. R. Kincaid in *The Porphyrin Handbook*, *Vol. 7*, 1st ed. (Eds.: K. M. Kadish, K. M. Smith, R. Guilard), Academic Press, San Diego, **2000**, pp. 225 – 291; b) T. G. Spiro, X.-Y. Li in *Resonance Raman Spectra of Heme and Metalloproteins*, 1st ed. (Ed.: T. G. Spiro), Wiley, New York, **1988**, pp. 1 – 38.
[22] a) L. A. Andersson, M. Mylrajan, E. P. Sullivan, Jr., S. H. Strauss, *J. Biol. Chem.* **1989**, *264*, 19099 – 19102; b) T. Kitagawa, Y. Kyogoku, T. Iizuka, M. I. Saito, *J. Am. Chem. Soc.* **1976**, *98*, 5169 – 5173; c) T. G. Spiro, R. S. Czernuszewicz in *Physical Methods in Bioinorganic Chemistry—Spectroscopy and Magnetism*, 1st ed. (Ed.: L. Que, Jr.), University Science Books, Sausalito, **2000**, pp. 59 – 119.
[23] T. G. Spiro, J. D. Stong, P. Stein, *J. Am. Chem. Soc.* **1979**, *101*, 2648 – 2655.
[24] X. D. Ding, A. Weichsel, J. F. Andersen, T. K. Shokhireva, C. Balfour, A. J. Pierik, B. A. Averill, W. R. Montfort, F. A. Walker, *J. Am. Chem. Soc.* **1999**, *121*, 128 – 138.
[25] E. M. Maes, F. A. Walker, W. R. Montfort, R. S. Czernuszewicz, *J. Am. Chem. Soc.* **2001**, *123*, 11664 – 11672.

